



GLOBAL JOURNAL OF RESEARCHES IN ENGINEERING: A
MECHANICAL AND MECHANICS ENGINEERING
Volume 14 Issue 7 Version 1.0 Year 2014
Type: Double Blind Peer Reviewed International Research Journal
Publisher: Global Journals Inc. (USA)
Online ISSN: 2249-4596 & Print ISSN: 0975-5861

Analysis of an NACA 4311 Airfoil for Flying Bike

By Amit Singh Dhakad, Pramod Singh & Arun Singh

Chhattisgarh Swami Vivekanand University, India

Abstract- The development of the wing has been always such that it should be able to produce the maximum lift due to the high pressure on the bottom surface and low pressure on the top surface of an airfoil. And these concepts clears that the flow of air/velocity of air will be low on the lower surface and higher on the upper surface of an airfoil. So, due to these differences in pressures and velocity the aerial can produce lift. Here to let fly the Bike in the air the Flat bottomed Airfoil has been chosen and usually the flat bottomed airfoil is called as the Clark Y and this has the feature as Maximum thickness of 11.7% at 28% chord and maximum camber of 3.4% at 42% chord.

Keywords: *NACA 4311 airfoil, flat bottomed airfoil, javafoil, clark Y.*

GJRE-A Classification : *FOR Code: 091399p*



Strictly as per the compliance and regulations of:



Analysis of an NACA 4311 Airfoil for Flying Bike

Amit Singh Dhakad^a, Pramod Singh^σ & Arun Singh^p

Abstract- The development of the wing has been always such that it should be able to produce the maximum lift due to the high pressure on the bottom surface and low pressure on the top surface of an airfoil. And these concepts clearly that the flow of air/velocity of air will be low on the lower surface and higher on the upper surface of an airfoil. So, due to these differences in pressures and velocity the aerial can produce lift. Here to let fly the Bike in the air the Flat bottomed Airfoil has been chosen and usually the flat bottomed airfoil is called as the Clark Y and this has the feature as Maximum thickness of 11.7% at 28% chord and maximum camber of 3.4% at 42% chord.

Keywords: NACA 4311 airfoil, flat bottomed airfoil, javafoil, clark Y.

I. INTRODUCTION

The wing considered is the flat Bottom (NACA 4311) which is a Clark Y type usually called just because it comes under the Flat bottomed surface airfoil and has the features of maximum thickness (t/c): 11.63% @ 30.81% and maximum camber of 3.54% @ 34.52% (when plotted for 81 points) And as in order to provide the maximum lift with minimum drag we will analyze the various kinds of airfoil using the airfoil analysis software called JAVAFOIL. And the main purpose of JAVAFOIL is to determine the lift, drag and the moment characteristics of airfoils. For this reason it uses a potential flow analysis module which is based on the higher order panel method (linear varying vorticity distribution), Since the drag force is referred as the energy loss property, so to minimize it, we will choose various airfoils to compare the best one. So, with the help of JAVAFOIL we will look over the various properties and characteristics of an airfoil.

a) Reason for the choosing of Clark Y type Airfoil is as follows:

i. Characteristics of Clark Y:

- Clark Y has a flat bottomed profile of an airfoil and is usually safe for gliding with lower pitch in the air.

Author a: Department of Mechanical Engineering, Christian College of Engineering and Technology, Chhattisgarh Swami Vivekanand University, Bhilai (Durg), C. G, India. e-mail: innovaamit@yahoo.co.in

Author σ: Department of Mechanical Engineering, Siddhaganga Polytechnic, Tumkur, Board of Technical Education, Bangalore-Karnataka, India. e-mail: licchi85@yahoo.co.in

Author p: Department of Mechanical Engineering, Sendur Polytechnic, Yashwant Nagar, Board of Technical Education, Bangalore-Karnataka, India. e-mail: arun.mars5@gmail.com



Fig 1 : (Clark YH wingroot of a Yak-18T)

b) Applications

Some representative aircraft that used the Clark Y and Yh are listed below:

- | Clark Y | Clark YH |
|---------------------------|--------------------------|
| • Ace Baby Ace | • Currie Wot |
| • Aeronca 50 Chief | • Hawker Hurricane |
| • Avia B.122 | • Ilyushin Il-2 |
| • Curtiss P-6 Hawk | • Mikoyan-Gurevich MiG-3 |
| • Fleet Fawn | • Miles Magister |
| • Heath Parasol | • Nanchang CJ-6 |
| • Lockheed Vega | • Polikarpov I-153 |
| • Long Henderson Longster | • Stolp SA-900 V-Star |
| • Monocoupe 90 | • Yakovlev Yak-18T |
| • Polikarpov R-5 | |
| • Spirit of St. Louis | |
| • Stinson Reliant | |
| • Waco UPF-7 | |

Here with the help of an Airfoil tool generator we can construct any profile of required data and can be experimented for results. The five Flat bottom airfoil (NACA-4311, 3310, 3310 with P= 38.6%), 2306, 2206 and Symmetrical airfoil NACA 2412 are generated through this software (Airfoil tool generator) Source: <http://www.airfoiltools.com/airfoil/naca4digit>

II. METHODOLOGY

a) Considering the type of airfoil for analysis on

- NACA 4311 (Flat Bottomed Airfoil)
- NACA 3310 with thickness: 38.6%, (Flat Bottomed Airfoil)
- NACA 3310 with thickness: 31.8%, (Flat Bottomed Airfoil)
- NACA 2306, (Flat Bottomed Airfoil)
- NACA 2206, (Flat Bottomed Airfoil)
- NACA 2412, (symmetrical Airfoil)

On analyzing the above airfoil (a-f) in JAVAFOIL, we have the result as

Table 1

Sl. no	Airfoil	Coefficient Of Lift	Coefficient Of drag	Coefficient Of moment
1.	NACA 4311	0.48101	0.01089	-0.09216
2.	NACA 3310 (p=38. 6%)	0.41505	0.00978	-0.08836
3.	NACA 3310 (p=31. 8%)	0.39486	0.01063	-0.07784
4.	NACA 2306	0.22477	0.00958	-0.04518
5.	NACA 2206	0.21175	0.00955	-0.03669
6.	NACA 2412	0.25889	0.01032	-0.05525

WHILE FOR CLARK Y (from JAVAFOIL) we have the result as:

Table 2 : (Javafoil analysis)

Sl.no	Airfoil	Coefficient Of Lift	Coefficient of drag	Coeff Of moment
1.	Clark Y (NACA 3411)	0.44560	0.01231	-0.09714

Table 3 : (Result from Gedser Simulation), A textbook on the thesis in Aeronautical Engineering

Airfoil	Operational	No roughness	Roughness	Difference	TSR	$C_{P, \max}$	Wind speed m/s
Operational	200 kW				4.4	0.32	8.5
NACA 4312		235 kW	210 kW	15 %, 5 %	4.4, 4.4	0.36, 0.34	8.5, 8.5
CLARK Y		218 kW	202 kW	9 %, 1 %	4.4, 4.4	0.33, 0.33	8.5, 8.5

Thus, on comparing the above table 1, 2 and 3, we have the best result from NACA 4311 due to the modification of Clark Y type airfoil for maximum lift and minimum drag.

b) Analysis of NACA 4311

Therefore, to analyze the airfoil for its characteristics and performance, a JAVAFOIL has been used which is an Aerodynamic software Source: (<http://www.airfoiltools.com/airfoil/naca4digit>) for the illustration of various aerodynamic properties.

c) Geometry

This is the first step in JAVAFOIL to obtain the required shape of an airfoil by giving the details of airfoil or by giving the coordinates and the airfoil will be developed selecting the create airfoil option.

Geometry | Modify | Design | Velocity | Flowfield | Boundary Layer | Polar | Aircraft | Options

Airfoil Geometry

Name:

Coordinates:

1.00000000	0.00000000
0.99862288	0.00038822
0.99407852	0.00154634
0.98653277	0.00345327
0.97602787	0.00607487
0.96262291	0.00936489
0.94639374	0.01326631
0.92743282	0.01771296
0.90584895	0.02263124
0.88176697	0.02794186
0.85532722	0.03356144
0.82668500	0.03940400
0.79600979	0.04538222
0.76348440	0.05140847
0.72930398	0.05739562
0.69367498	0.06325766
0.65681399	0.06891027
0.61894650	0.07427128

Clear

decimal digits:

Create an Airfoil:

Family:

Number of Points: [-]

Thickness t/c : [%]

Thickness Location xt/c : [%]

Camber f/c : [%]

Camber Location xf/c : [%]

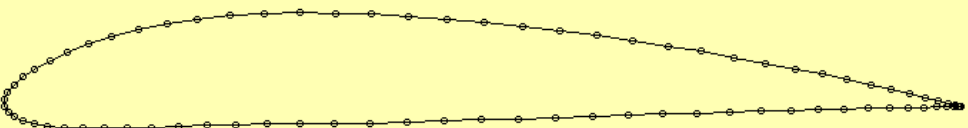
[%]

☒ Modify NACA section to have closed trailing edge

This is a general purpose airfoil series

Create Airfoil

Airfoil Shape



For later analysis the trailing edge should be closed.

Update View | Copy (Text) | Paste (Text) | Open... | Save... | Print... | Compare...

Fig 2: Geometry card: (here we observe the required airfoil in 2d view in a scale of 1/1)

Modification

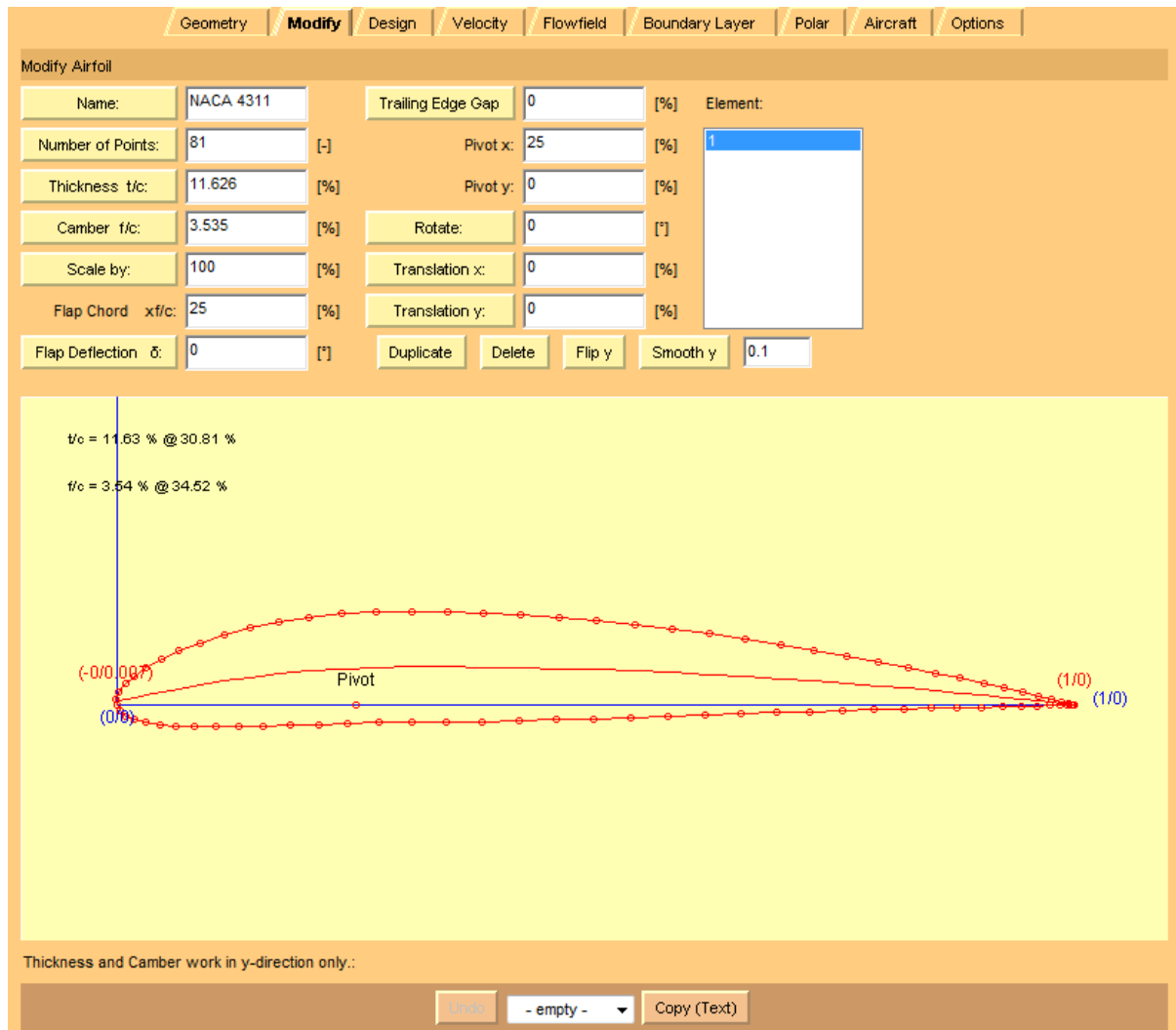


Fig 3 : (Here in the second part of the analysis we have the modified 2D Dimensional view of the Clark Y Airfoil in a scale of 100mm with the trailing edge gap as zero in order to get the smooth aerodynamic nature and named as NACA 4311. This card can be used to perform various modifications to the airfoil geometry. Where we can see the center red line which is called camber line, while the upper and lower dotted line are upper and lower surfaces. Also upper and lower surface forms maximum thickness, which is given as $t/c = 11.63 \% @ 30.81 \%$ and the maximum camber of $f/c = 3.54$ is located at 34.52% of the chord length. While the points at trailing edge are intersecting with the ground)

So, after modification we get properties of airfoil on modified screen are

- Smoothy Y = 0.1, which describes that the airfoil has a smooth spline curve.
- (Pivot x=25%) horizontally at red point describes that the angle of attack of the airfoil is always change by rotating the section around the pivot point specified on the Modify card.

d) Design

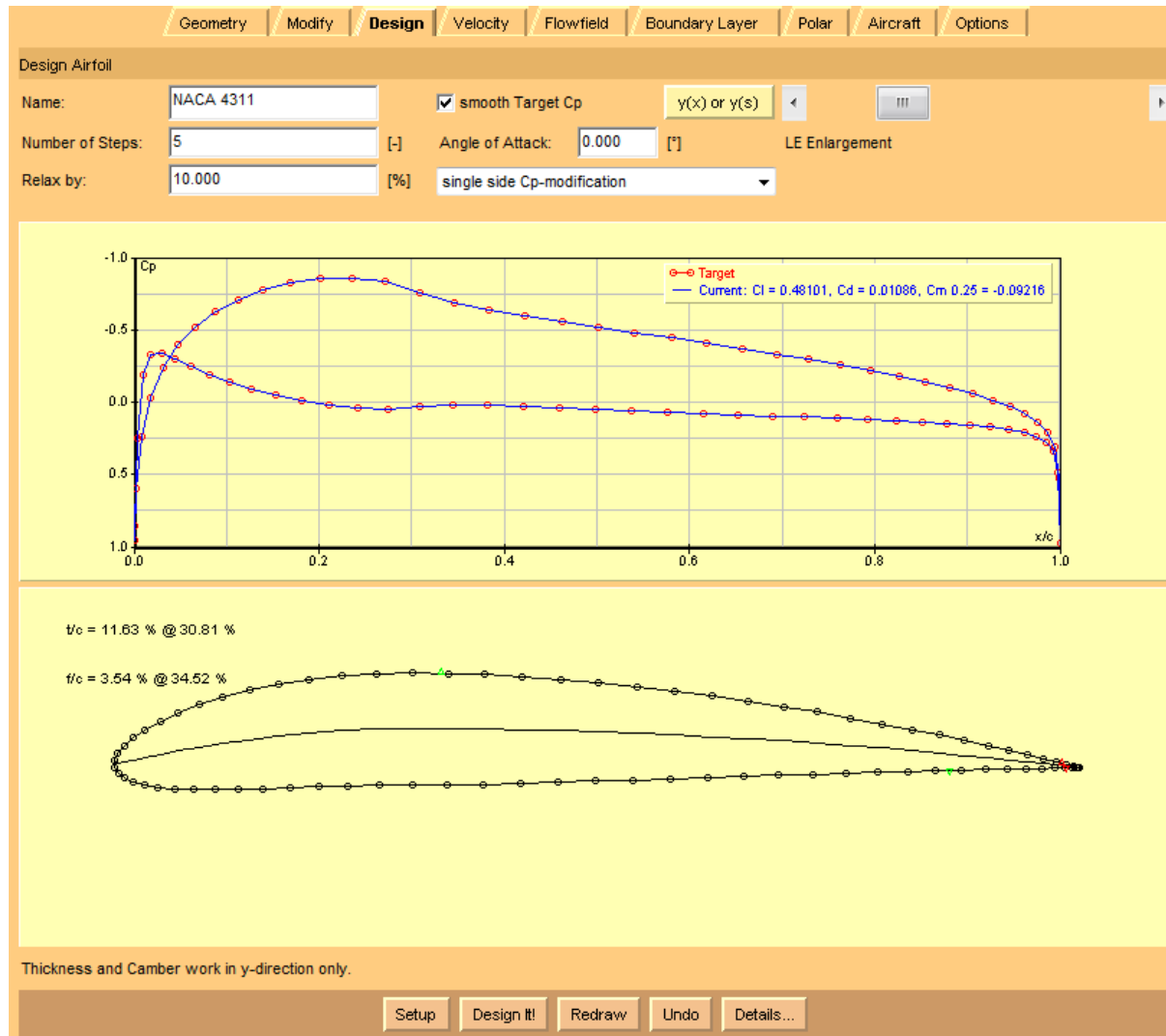


Fig 4 : (Here we can see the 2D Dimensional design of the NACA 4311 Airfoil, and it is delivering a lift of (Coefficient of lift) = 0.48101 and Coefficient of drag as 0.01086 at an angle of attack = 0° , while the graph shows the coefficient of pressure along the length of the chord(c))

- Here from the above (figure 4) we see that a graph is plotted for the airfoil and the upper surface is having the coordinates in negative mostly just because airfoil is experiencing a negative pressure and the lower surface is having a positive coordinates mostly just because it is experiencing a positive pressure which is responsible for the lift of an airfoil.

While, $\frac{L}{D} = \frac{C_l}{C_d}$ ratio gives Glide Ratio of the flight

e) Velocity

After design first it will calculate the distribution of the velocity on the surface of airfoil which can be integrated to get the lift and the moment coefficient. Number for different angle of attack.

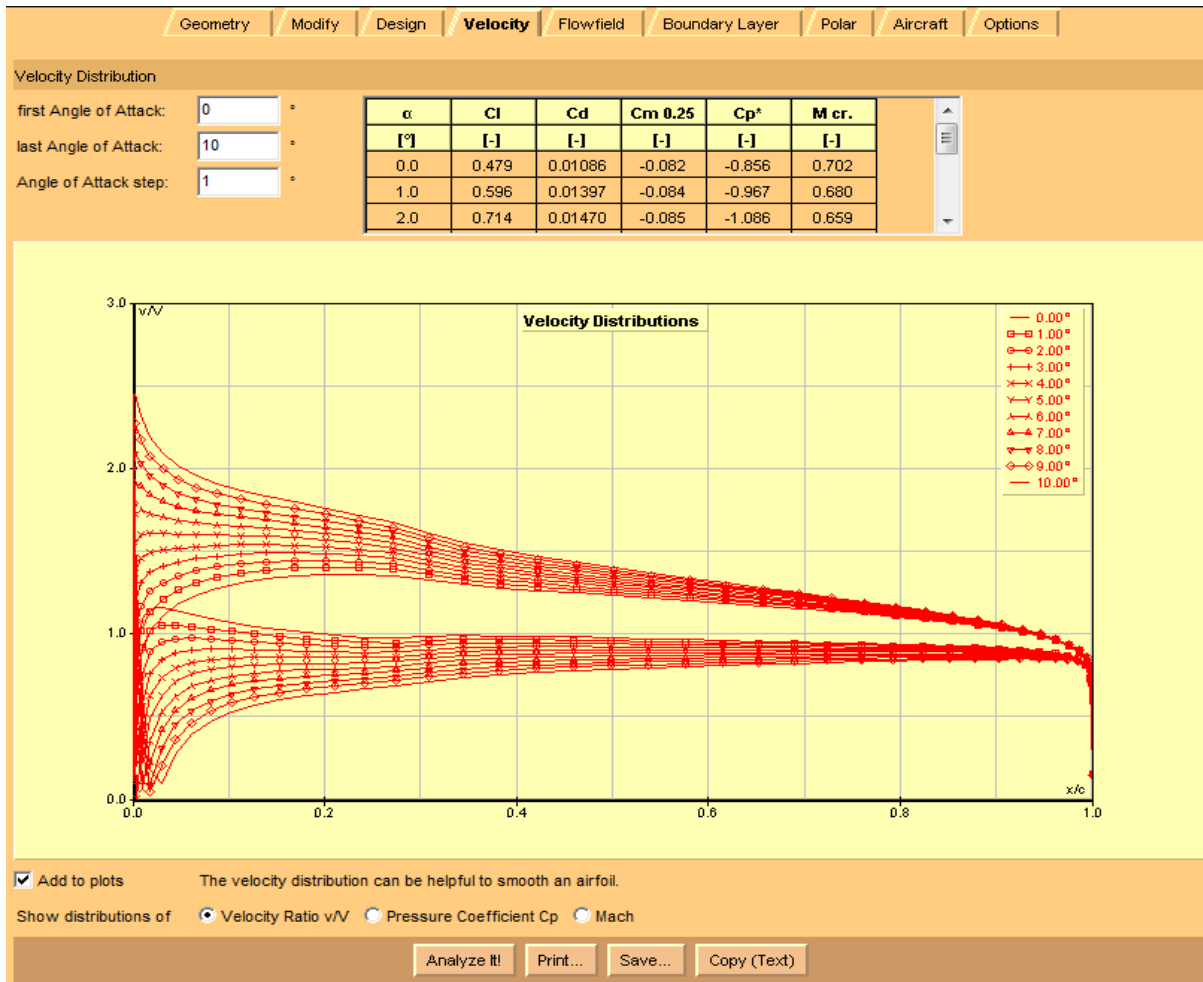


Fig. 5: (Velocity distribution past a NACA 4311 at an angle of attack of 10°. The results are for free flow.)

Therefore, the analysis on the velocity provides the information about the behavior of the airfoil which varies with the angle of attack. Hence from the above figure of Velocity distributions we can see that how it has behaved along the length of an airfoil for different angles. Also we can see the coefficient of lift (C_l) and Coefficient of drag (C_d) along with the pitching moment (C_m), coefficient of pressure (C_p) and Mach number (M_{cr}).

So, here we get the velocity distribution over airfoil (NACA 4311) for 10° of angle of attack in 10 steps which is shown by the ten upper line and ten lower line indicated on the right hand side top corner of the figure 5. While the (0-0) is the velocity distribution on the surface, where we can see that the velocity distribution is low at the stagnation point as it had dropped downwards due to the high pressure and again the velocity is much high in the upper surface than lower surface and it has again dropped down in the trailing edge without overlapping of upper and lower velocity

distribution profile and also it suggest that it is a laminar flow since no overlapping of profile is noticed. And the coefficient of lift (C_l) and drag (C_d), pitching moment (C_m), and critical coefficient of pressure (C_p) are increasing for every 10° angle of attack. Rather the Mach number (M_{cr}) is decreasing for every 10° angle of attack.

While, $M_{0.25}$ (Nm) is the pitching moment at 25% chord point.

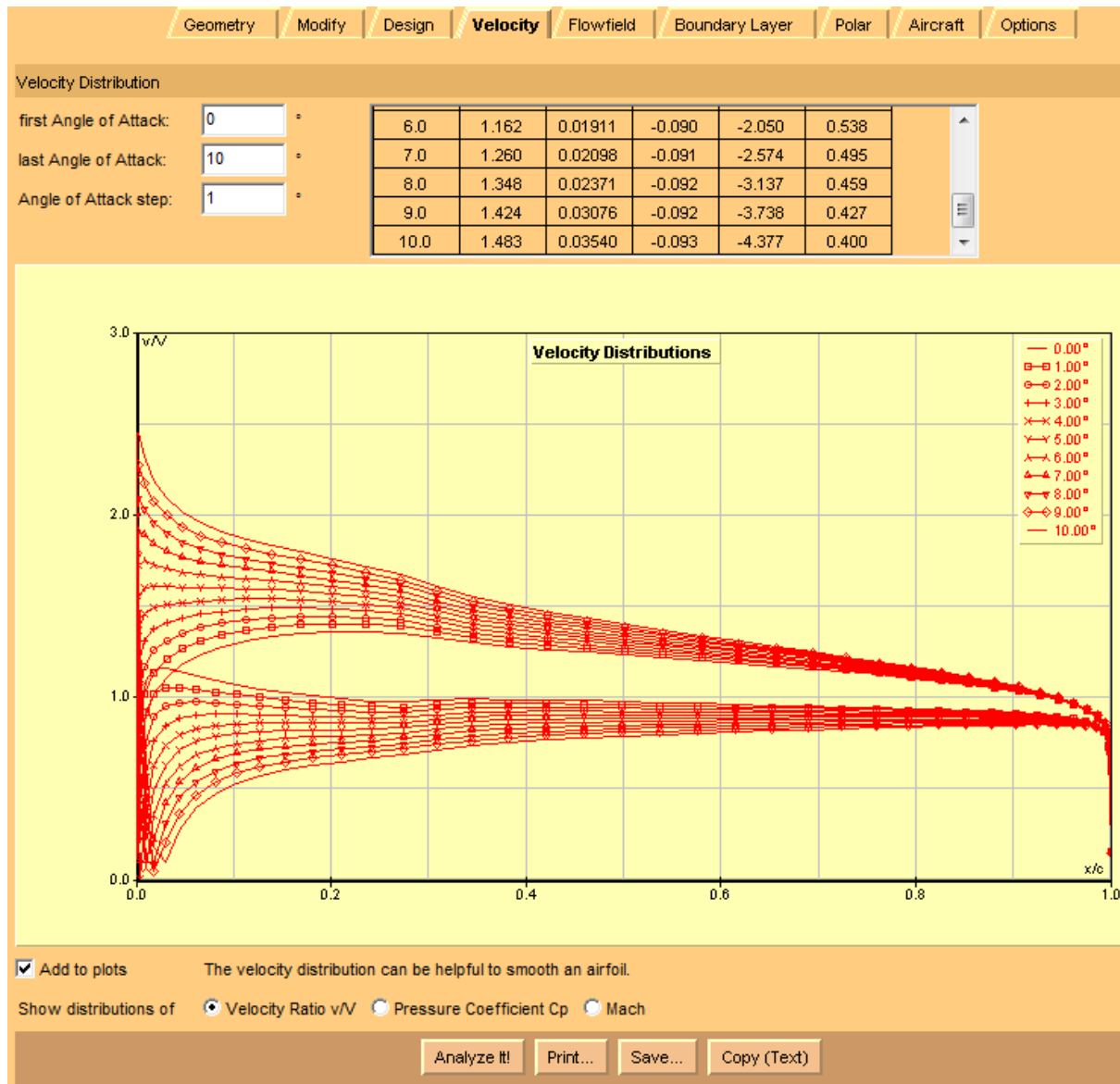


Fig 6 : (Velocity distribution for 10° angle of attack with different characteristics of (C_l), (C_d), (C_m) and Mach number

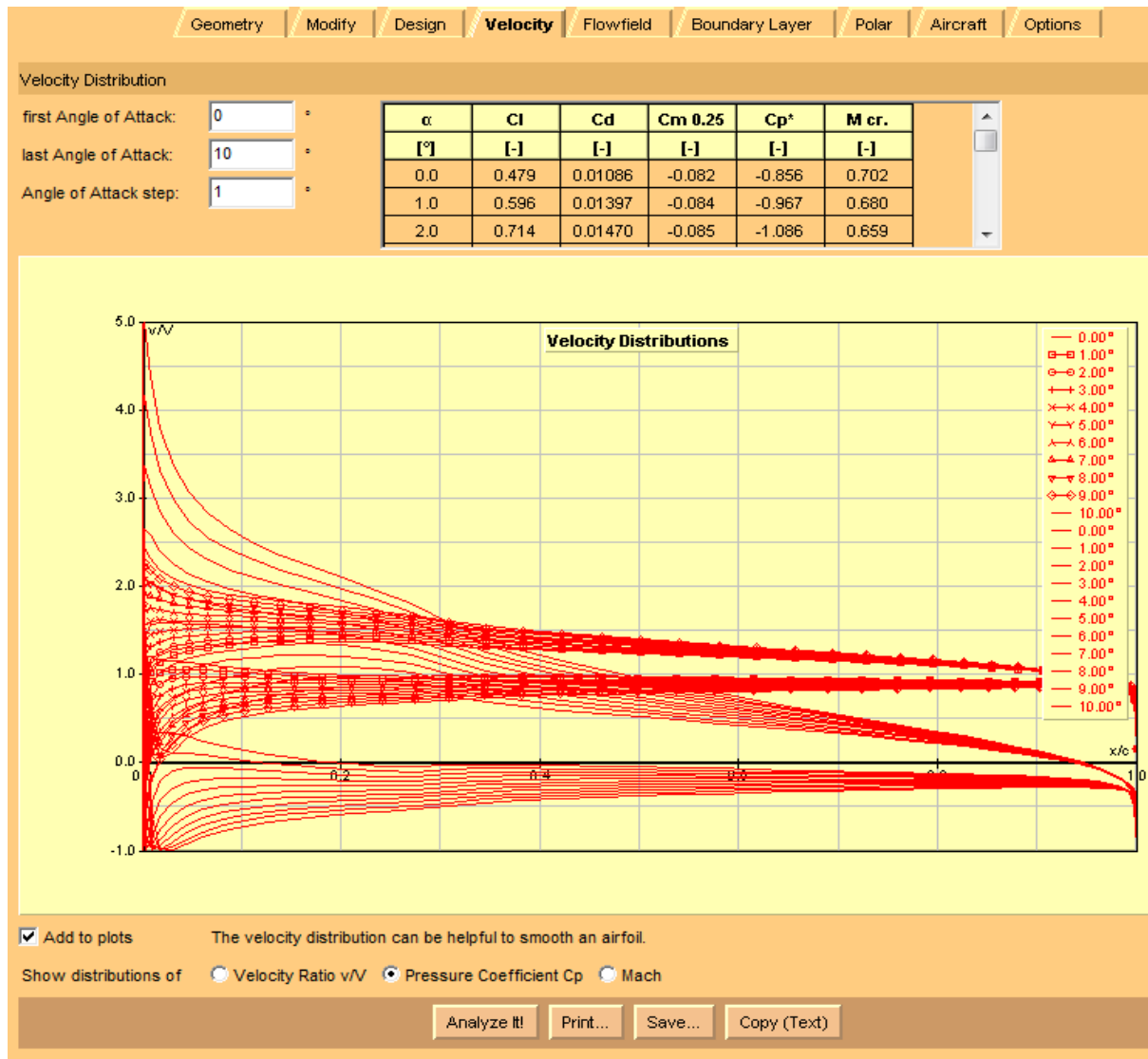


Fig 7 : (Velocity distribution profile with the pressure coefficient)

Therefore from the figure 7, we can see the pressure coefficient in a thin red lines for ten different angle of contact. And the Critical mach number for 0° is 0.702 and for the 10° the mach number 0.400. Hence the mach no is less than 0.8 so it concludes that the flight is subsonic. While the pressure are low in the upper surface of airfoil and high on the lower surface which creates the lift.

f) Mach Number

Mach number (M or Ma) is the ratio of speed of an object moving through a fluid and the local speed of sound.

$$M = \frac{v_{\text{object}}}{v_{\text{sound}}}$$

Where, v is the velocity of the source relative to the medium and v_{sound} is the speed of sound in the medium.

Table 4 : (General Plane Characteristic)

Regime:	Mach	Mph	km/h	m/s	General plane characteristics
Subsonic	<0.8	<610	<980	<270	Most often propeller-driven and commercial turbofan aircraft with high aspect-ratio (slender) wings, and rounded features like the nose and leading edges.

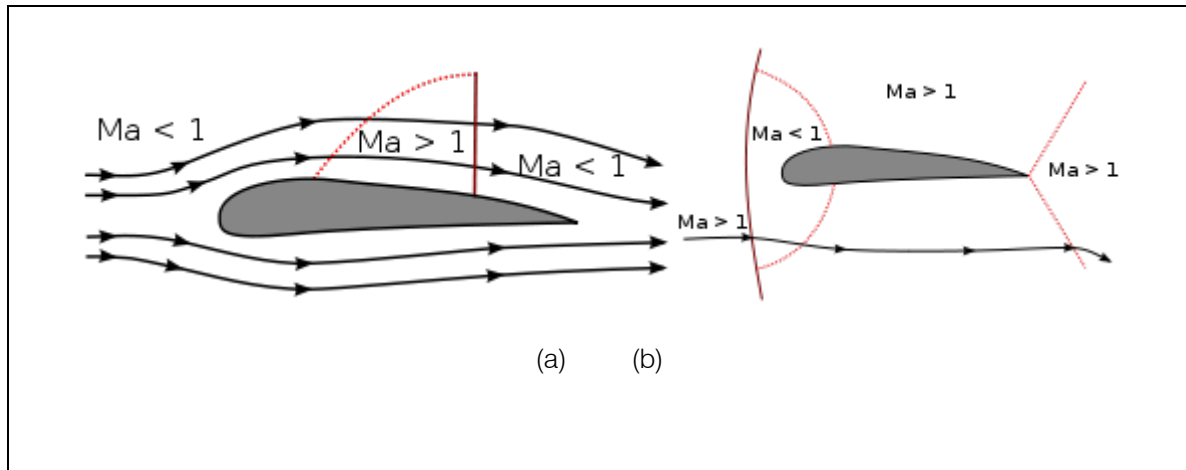


Fig. 8 : Mach number in transonic airflow around an airfoil; $M < 1$ (a) and $M > 1$ (b)

g) Thus from Figure 5, 6 & 7

- One can compare the velocity distribution for any angle of attack without and with ground in effect.

h) Flowfeild

Here in (Figure 9) the flow can be seen around the airfoil considering the angle of attack as 10° and with the boundary layer around an airfoil, it also includes the friction to show the boundary layer to result the exact behaviour of an airfoil as in practical. Where the rectangular grid is showing the local velocity points. And these calculation uses the vorticity distribution on the surface and neglects friction which leads to no separation flow or a wake behind the airfoil. And the streamlines are calculated from the software with the help of Runge Kutta method and Streamlines around the submersed airfoil can be seen through the blue continuity lines, while the black tufts are the black discontinued dashes.

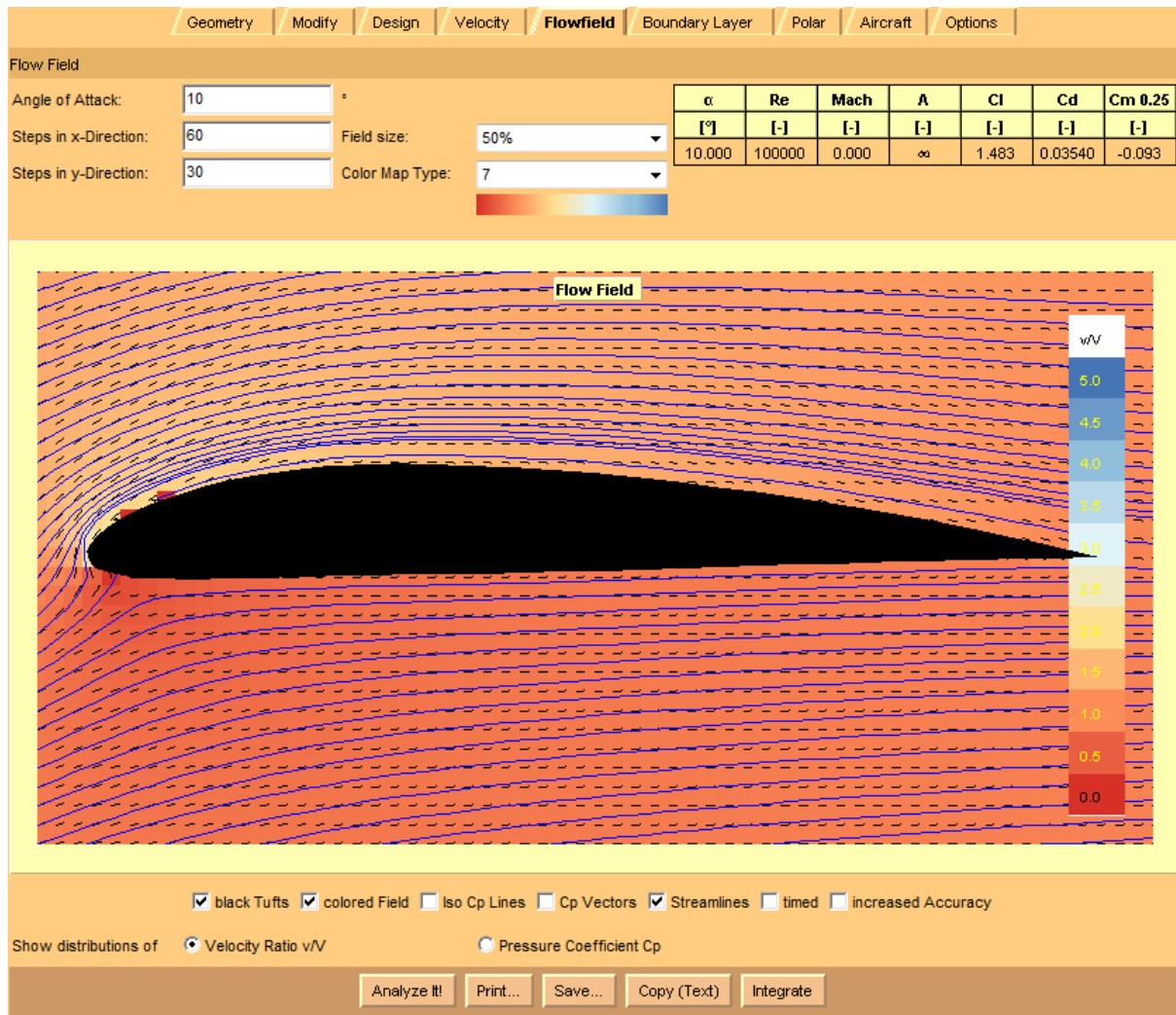


Fig. 9 : Streamlines around the submersed hydrofoil (note that image is clipped at $y=0$) but the generated surface wave are extending above this border

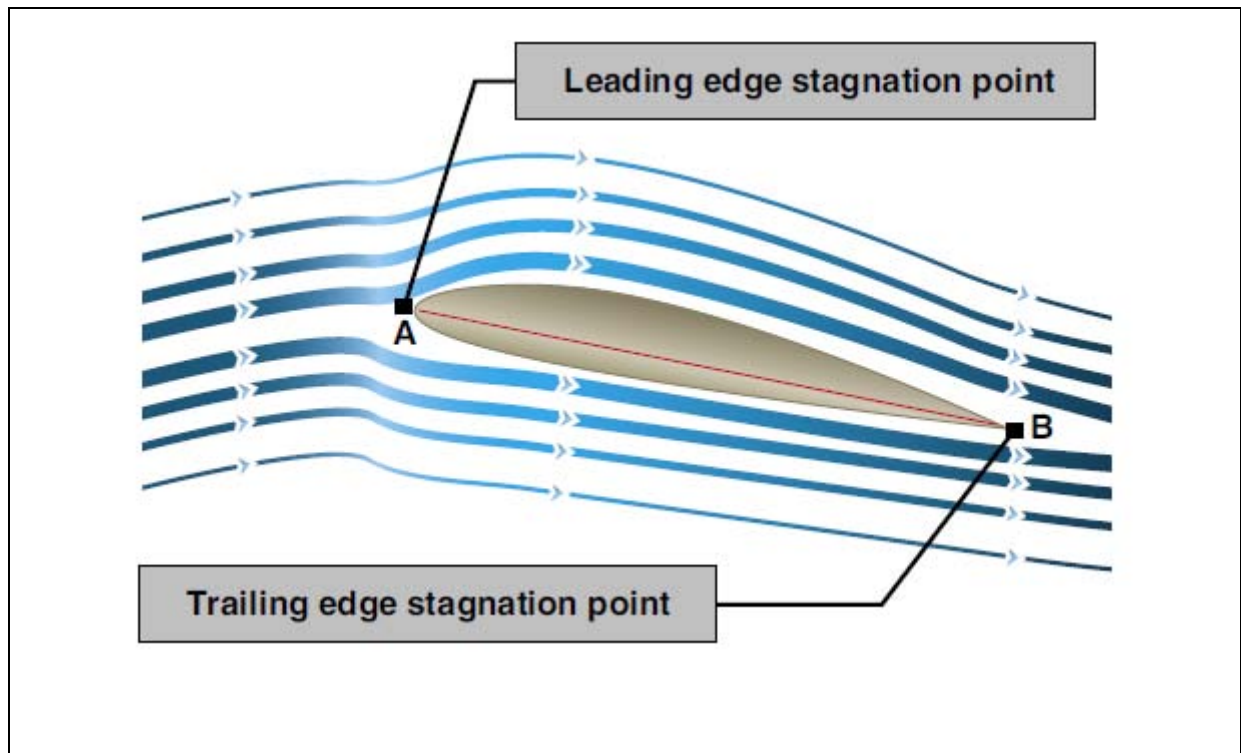


Fig. 10 : (stagnation points)

i) *Stagnation Point*

A *stagnation point* is a point in a flow field where the local velocity of the fluid is zero.

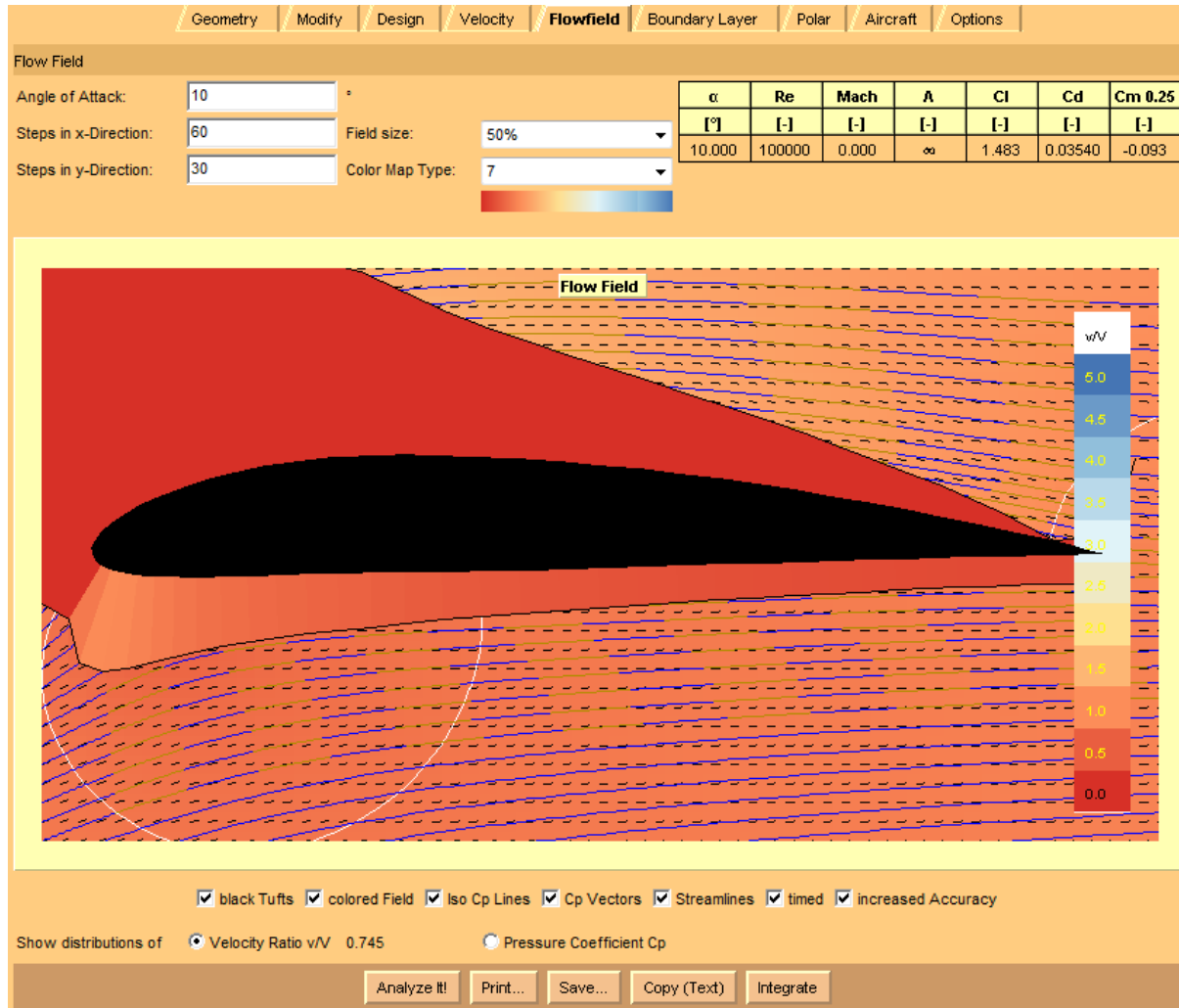


Fig. 11 : (The velocity ratio is zero at the Red location for which the v/V is given as 0.0 at the stagnation point)

j) *Pressure Distribution*

It has been determined that as air flows along the surface of a wing at different angles of attack there are regions along the surface where the pressure is negative, or less than atmospheric, and regions where the pressure is positive, or greater than atmospheric. This negative pressure on the upper surface creates a relatively larger force on the wing than is caused by the positive pressure resulting from the air striking the lower wing surface.

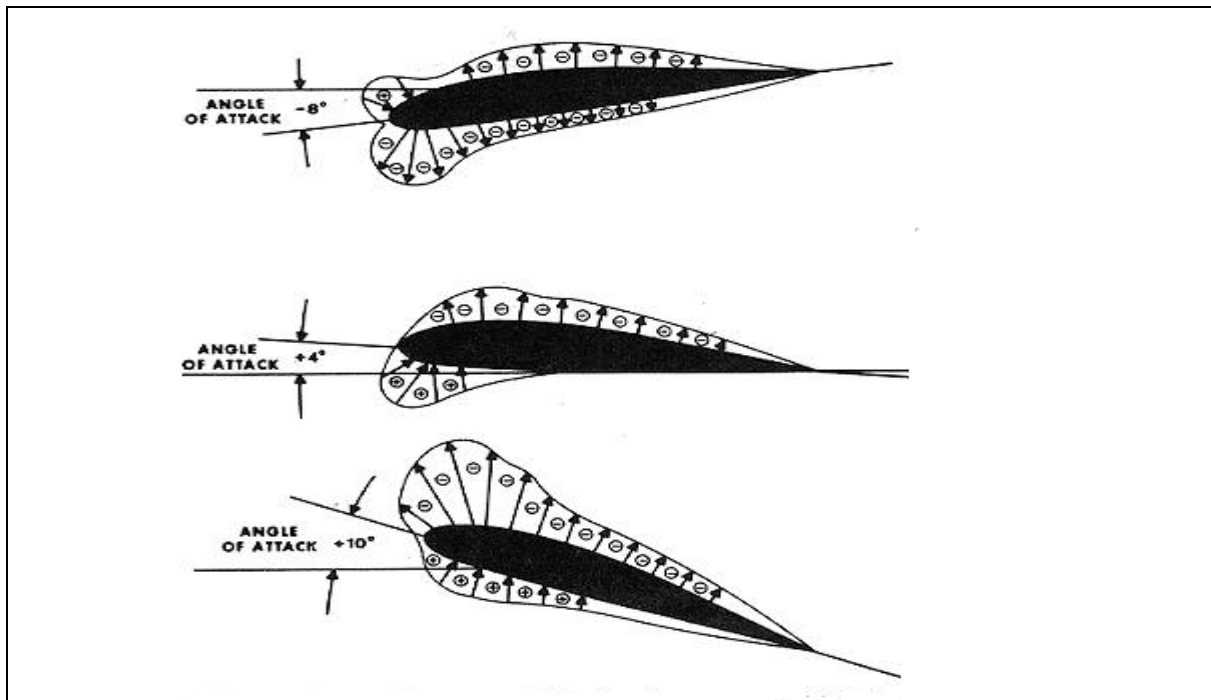


Figure 12 : Pressure distribution on an airfoil

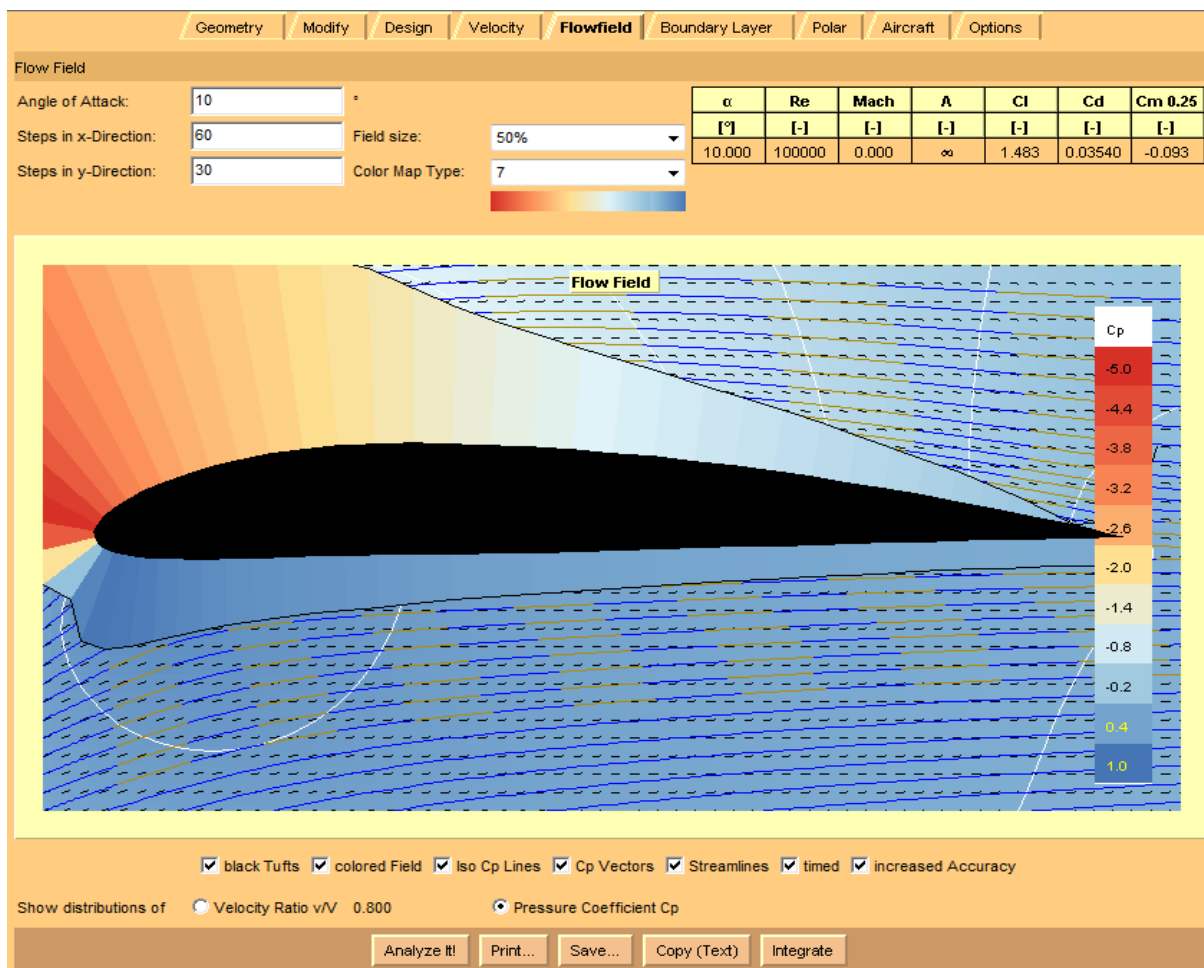


Fig. 13 : (Pressure distribution around airfoil)

While the pressure distribution is described in terms of Pressure coefficient and from the figure we can see the positive pressure and negative pressure along the length of an airfoil. Because the velocity of the flow over the top of the airfoil is greater than the free-stream velocity, the pressure over the top is negative.

Therefore here (from figure 13), we have the centre of pressure at the yellow point/region and we can read the pressure as Coefficient of pressure as (-2.0), similarly we can read the positive pressure which is responsible for the lift of an airfoil as $C_p = 1.0$ indicated

in blue color while the negative pressure can be read which is around the upper surface of an airfoil.

k) Boundary Layer

The boundary layer analysis describes the behaviour of an airfoil around it with the flow of air. The boundary layer module works best in the Reynolds number regime between 500'000 and 20'000'000. During the way towards the trailing edge, the method checks, whether transition from laminar to turbulent or separation occurs.

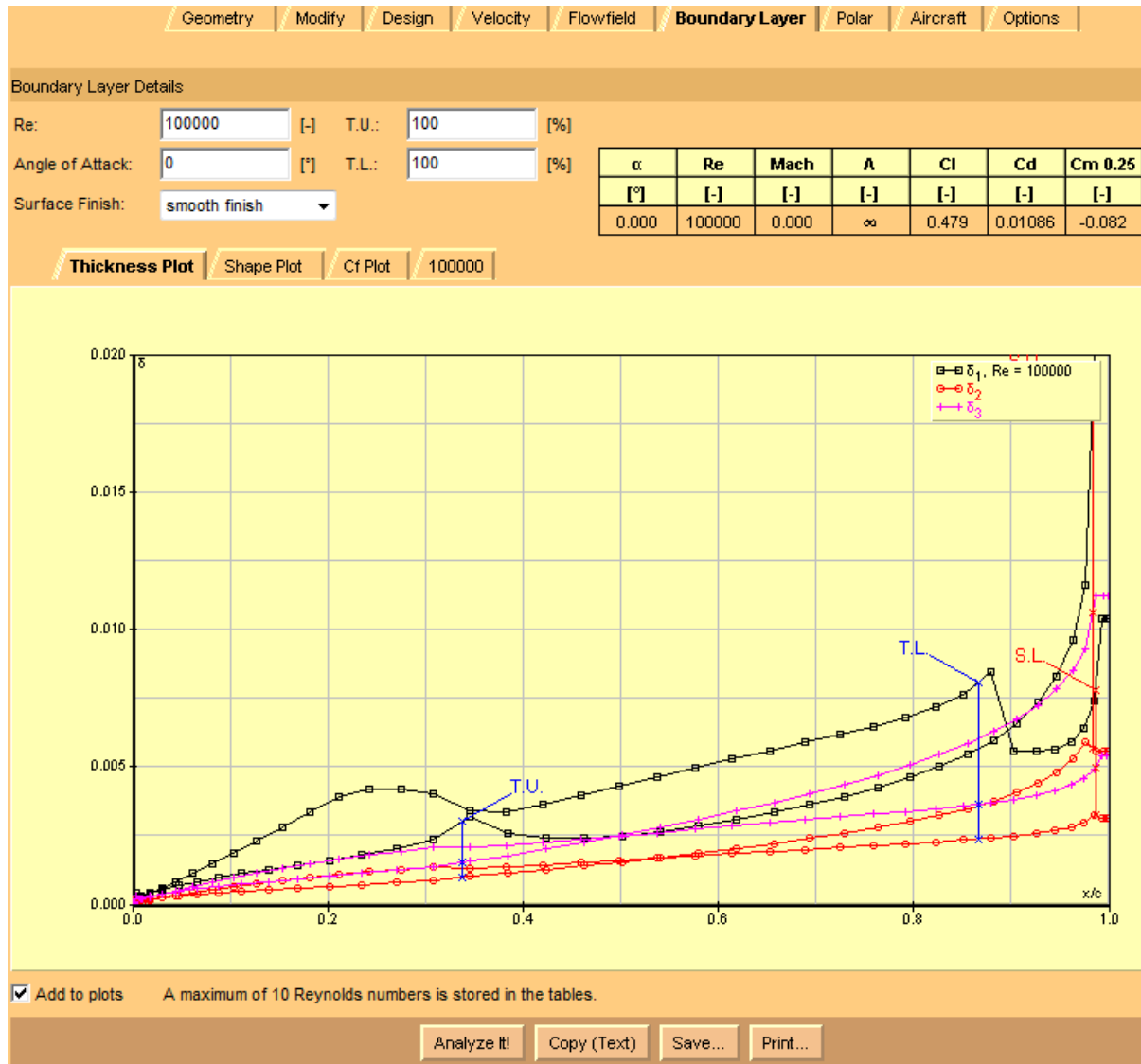


Fig. 14 : Analyzed boundary layer of NACA 4311

Therefore (from figure 14), we see that for δ_1 , δ_2 and δ_3 the blue line is indicating transition of flow from laminar to turbulent on the upper layer of the airfoil surface (TU) and transition of flow from laminar to turbulent on the lower layer of the airfoil surface (TL) while (SL) is indicating the turbulent separation of the flow near the end of the trailing edge.

Where,

- δ_1 (m) is the displacement thickness of boundary layer is the distance by which a surface would have to be moved in the direction perpendicular to its normal vector away from the reference plane in an inviscid fluid stream of velocity u_0 to give the

same flow rate as occurs between the surface and the reference plane in a real fluid.

- δ_2 (m) is momentum thickness of boundary layer is the distance by which a surface would have to be moved parallel to itself towards the reference plane in an inviscid fluid stream of velocity u_0 to give the same total momentum as exists between the surface and the reference plane in a real fluid.
- δ_3 (m) is energy thickness of boundary layer
- T is transition laminar-turbulent
- S is turbulent separation
- U is upper surface
- L is Lower surface
- A *shape factor* is used in boundary layer flow to determine the nature of the flow.

$$H = \frac{\delta^*}{\theta}, \text{ Note } \delta^* = \delta_1 / \delta_3 \text{ and } \theta = \delta_2$$

Where, H is the shape factor, δ^* is the displacement thickness and θ is the momentum thickness. The higher the value of H , the stronger the adverse pressure gradient. A high adverse pressure gradient can greatly reduce the Reynolds number at which transition into turbulence may occur.

- $H_{12} = \delta_1 / \delta_2$ is the shape factor of boundary layer and $H_{32} = \delta_3 / \delta_2$ is the shape factor of boundary layer, C_f is the local skin friction coefficient.

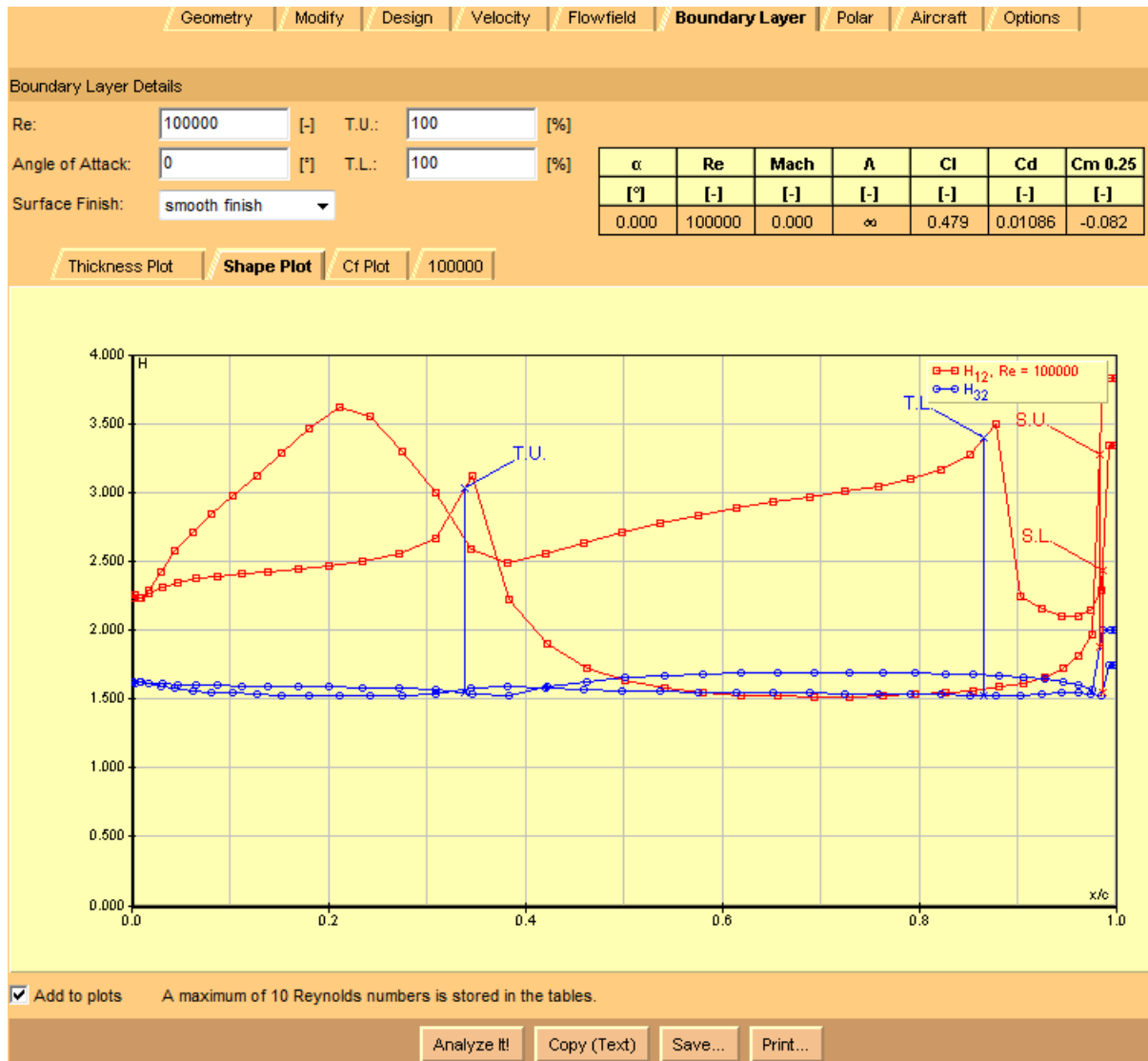


Fig. 15 : Flow state graph on airfoil NACA 4311

Pressure gradient is high (red line at point $H_{12} > 3.5$ for the Reynolds no. Here (from figure 18) it can be observed that for the maximum thickness of the airfoil, number (Re) = 100000. Also we can see the for the H_{32}

Where,

$H_{32} < 1.51509$ will have the laminar flow and $H_{12} < 1.46$ will have the turbulent flow, which can be observed from the figure 18, at TU, TL and SU, SL. The blue line is indicating transition of flow from laminar to turbulent on the upper layer of the airfoil surface (TU) and transition of flow from laminar to turbulent on the lower layer of the airfoil surface (TL) while (SL) and (SU) is indicating the turbulent separation of the flow near the end of the

trailing edge in the lower and upper surface of NACA 4311 in the both cases of H_{12} and H_{32} .

Table 5 : Shape factor boundary layer condition

Flow State	Separation assumed when
Laminar	$H_{32} < 1.51509$
Turbulent	$H_{12} < 1.46$

Also shape factor displacement thickness/ momentum thickness has the relation as

$$H_{12} = \frac{\delta_1}{\delta_2}$$

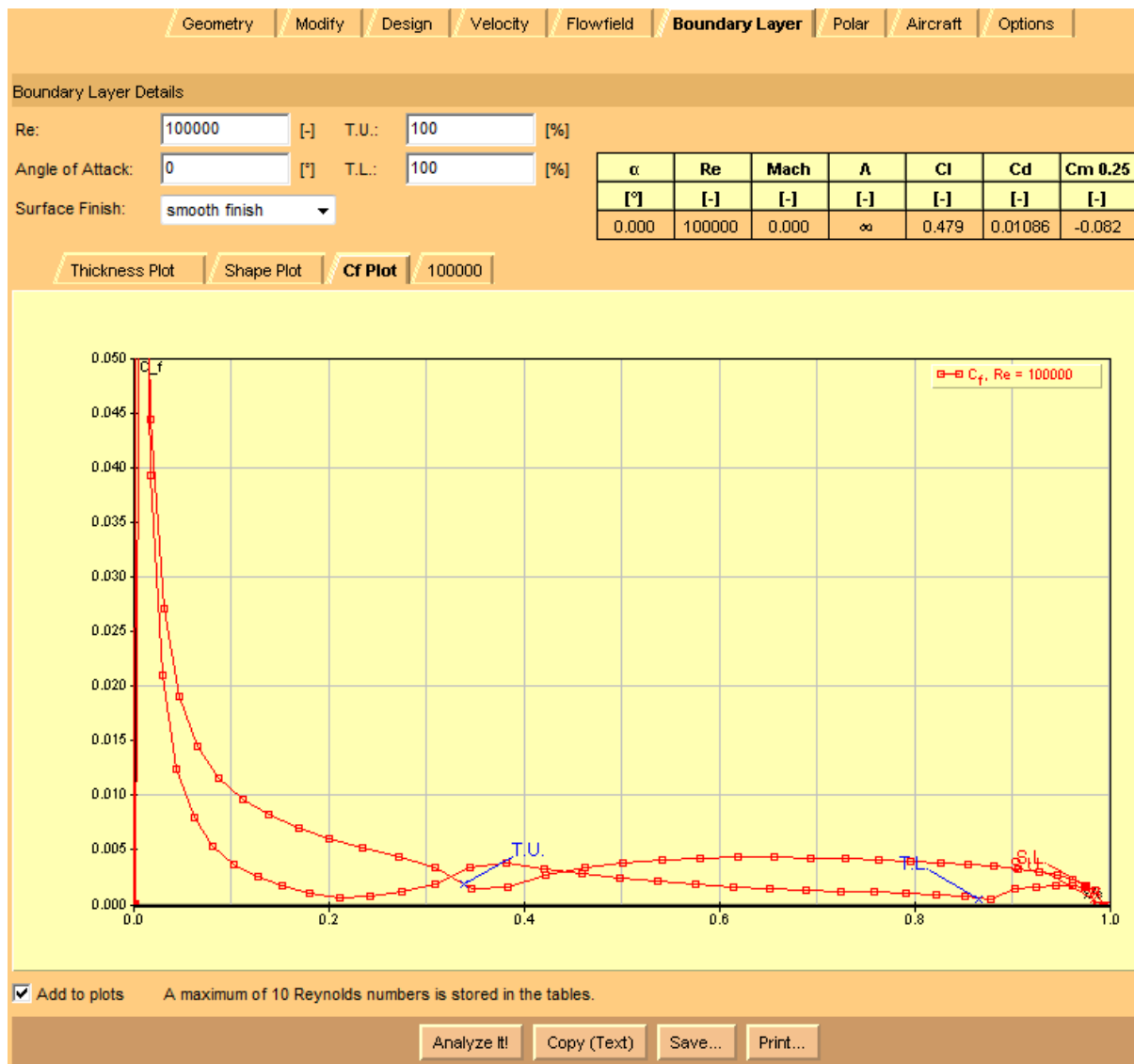


Fig. 16 : (local skin friction coefficient)

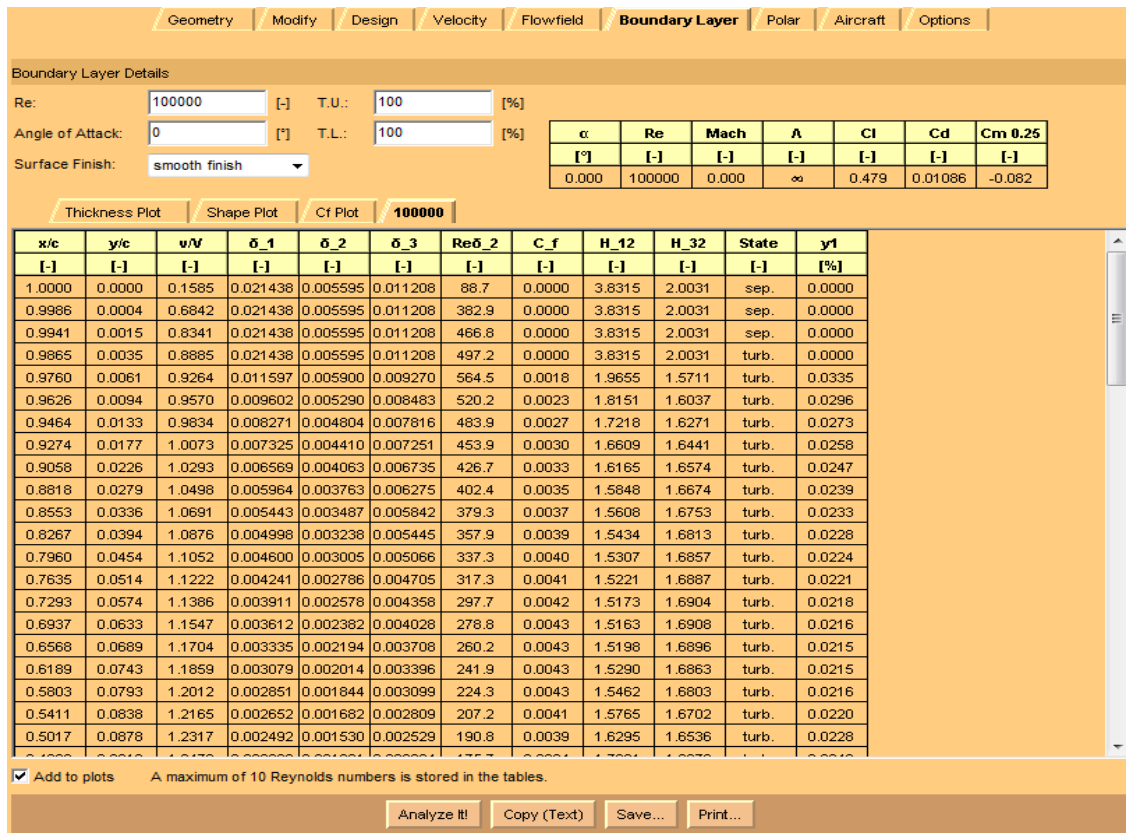


Fig. 17: (different value of calculated properties for the boundary layer)

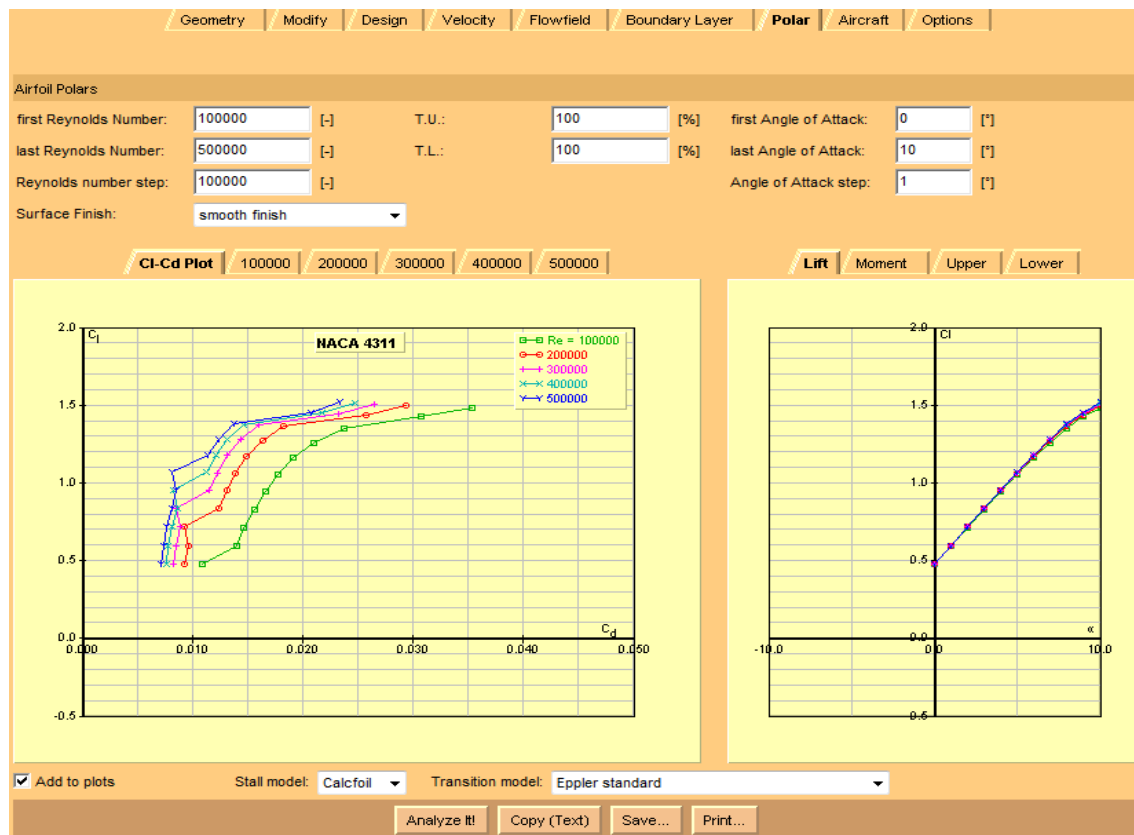


Fig. 18: (Lift versus drag coefficient polars for a NACA 4311 airfoil and wings of different aspect ratio)

The graph above shows the effect of lift over drag coefficient. Starting with infinite aspect ratio (aspect ratio = 0 on the Options card). It can be clearly seen, that for five Reynolds number (Re) the lift is increasing for larger value of (Re). As the lift will be maximum if the flow of air around the airfoil will be maximum.

l) Polars for Constant Wing Loading

The lift coefficient of any body depends on the speed because the wing loading is usually fixed during flight – flying at low lift coefficients results in high speeds

(and high Reynolds numbers) and vice versa. Therefore the operating points during flight would slice through a set of polars having constant Reynolds numbers. It is possible to create polars more closely related to the conditions during flight. This would require adjusting the wind speed to each lift coefficient, which is cumbersome and expensive in a wind tunnel, but feasible in a numerical tool like J AVAFOIL. And here we use the Aircraft card to calculate polars for a given wing loading.

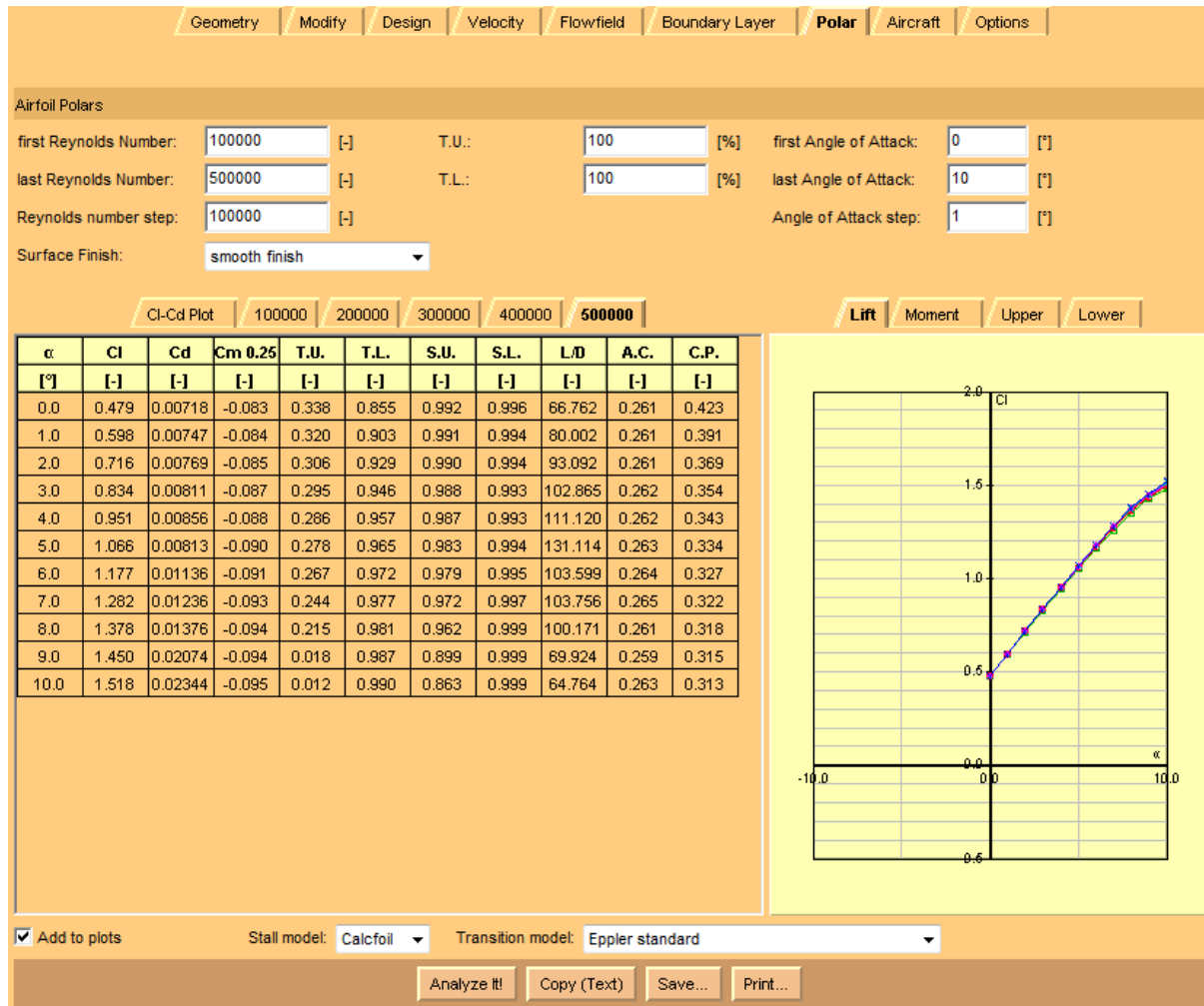


Fig. 19 : (polar condition of flight for different Reynolds number (Re))

m) Aircraft

The Polars card analyzes the airfoil for constant Reynolds numbers. For an aircraft in flight the lift coefficient depends on the flight speed and hence on the Reynolds number.

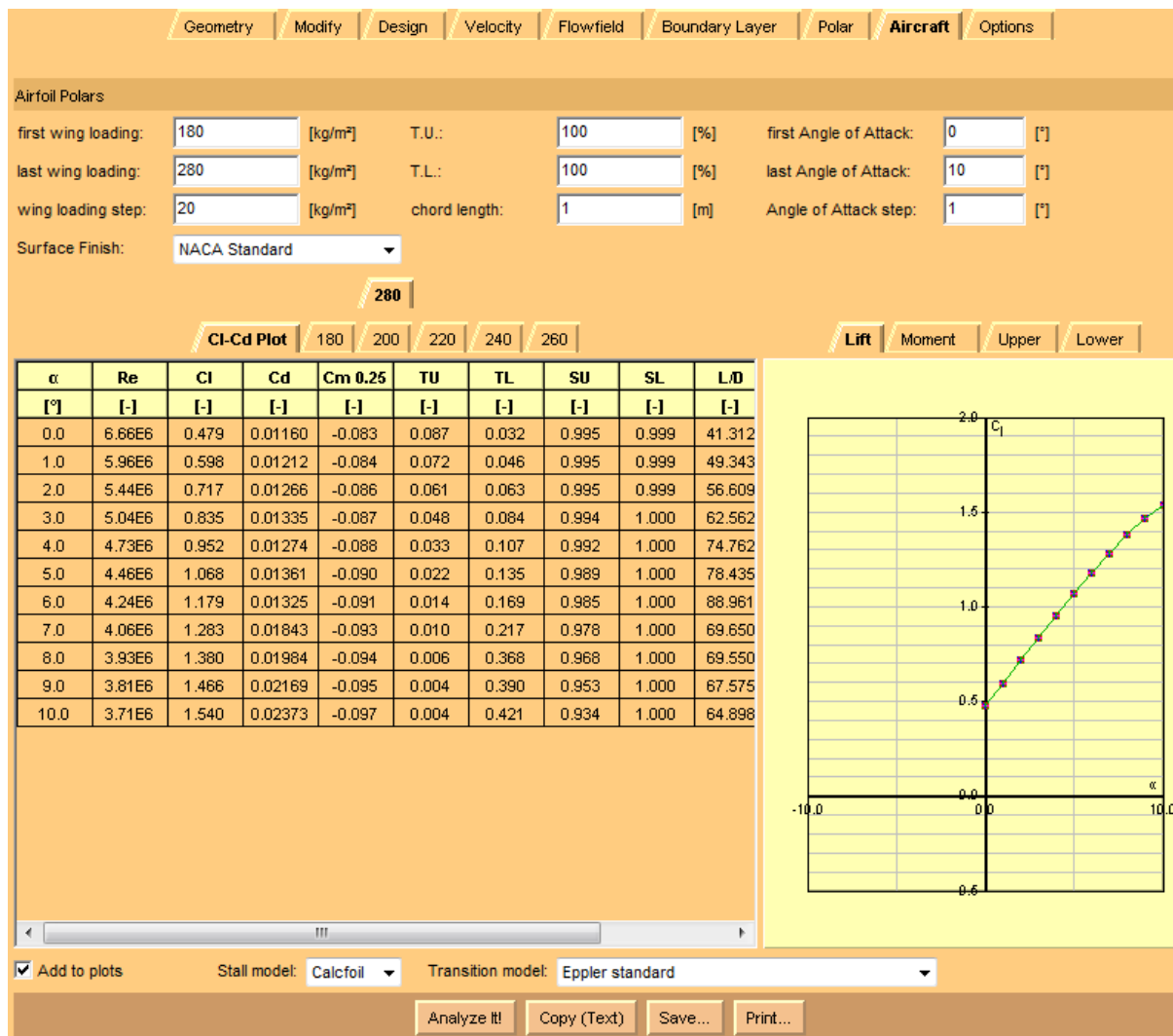


Fig. 20 : (Wing loading condition for maximum weight and result for different angle of attack)

Notes

- To check the airfoil for different angles of attack, one can analyze complete polar for different angles of attack and Reynolds numbers. The angle of attack is changed by rotating the airfoil around the point (0.25/0), which will change the height of the airfoils 25% chord point above ground somewhat.

n) Option

The aspect ratio is used for an approximate correction of the results on the Polar and Aircraft cards for a finite wing.

Geometry Modify Design Velocity Flowfield Boundary Layer Polar Aircraft Options

Adjust the desired Option(s).

JavaFoil

Version 2.21 - 1 March, 2014.

Copyright ©2001-2014 © Martin Hepperle

Translation to French by Giorgio Toso.
Translation to Italian by Giorgio Toso.
Translation to Spanish by Israel Gandara.
Translation to Portuguese by João Alveirinho Correia.
Translation to Finnish by Matti Hyötyniemi.
Translation to Dutch by Henri Rommelse.

Your current system settings
Your user name is admin.
You are running Windows 7, Java version 1.7.0_67, Java memory is 15872 / 253440 kB.
System language code is en.
selected country is India, selected language is English.

Country Settings: India (decimal character is: '.', path separator: ',')

Density ρ : 1.2210 [kg/m³]

Kinematic Viscosity ν : 0.000014607 [m²/s]

Speed of Sound a : 340.29 [m/s]

Mach: 0

Aspect Ratio: 0

Height / Span: 0.5 (ground effect only)

sweep angle: 0.0 °

Character Set: windows-1252 used for files and clipboard exchange

☒ unbounded flow field ☐ ground effect (ground at y=0) ☐ Froude effect (free surface at y=0)

Save... Open... Script ☐ Clear preferences on exit

Fig. 21 : (Setup values for the analysis of Airfoil data)

III. CONCLUSION

From the analysis program in Java Foil for an NACA 4311 it is observed that on the final loading of both front and rear wings, the result is positive and there is no drop in coefficient of lift for angle of attack considered ($\alpha=10^\circ$) with the consideration of ground effect with a air density of 1.2210 kg/m³ and kinematic viscosity (ν) of which results for the unbounded flow for the swiipe angle of 0.0 because the wing considered is uniform in cross section (rectangular) behaving under speed of sound ($a=340.29$ m/s) as it result the mach number.

REFERENCES RÉFÉRENCES REFERENCIAS

1. Amit Singh Dhakad, and Pramod Singh. "Flying bike concept." *International Research Journal of Mechanical Engineering*, Vol 1, PP. 001-011. March 2014.
2. Amit & Arun Singh. "Power Requirement for Flying Bike." *International Journal of Innovative Research and Development* [Online], 3.5 (2014): n. pag. Web. 17 Jun. 2014.
3. Mehrdad Ghods. "Theory of wings and wind tunnel test of a NACA 2415 airfoil" Technical

- Communications for Engineers, The University of British Columbia, pp-1-13, July 23, 2001.
4. Christopher A Lyon, Andy P Broren, Philippe Gigu'ere, Ashok Gopalarathnam, Michael S Selig (1997). Summary of low speed airfoil data, soar Tech publications, Virginia.
 5. Dava Newman, Pete Young (2004). Introduction to aerospace and Design-Chapter 4, Massachuetts Institute of Technology, pp.1-17.
 6. Jonathan Densie, Model Aircraft Design, Defence Science and Technology organisation-Researching Aircraft Flight Mechanics, Melbourne http://www.-concept2creation.com.au/xstd_files/Jon%20Dansie%20Model%20Aircraft%20Design.pdf.
 7. Mustafa Cavcar, e-material (2005): The International Standard Atmosphere (ISA), Anadolu University, 26470 Eskisehir, Turkey. pp. 1-7
 8. Wikipedia on aircrafts (lift, thrust, propellers and theory of flight) <http://en.wikipedia.org/wiki/Aircraft>
 9. Wing Design e-Book (2010). National Aeronautic and Space Administration, Museum in a box series - Aeronautics Research Mission Directorate.
 10. Fan wing manned aircraft project (<http://www.-fanwing.com/fanwing%20manned%20aircraft%20project%202013.pdf>)
 11. B. L Singhal, Fluid Machinery, Tech-Max Publications, ISBN 978-81-8492-805-1, First edition, (2011).
 12. Airfoil generator (software), www.airfoil.com/-airfoil/naca4digit
 13. Air properties, $M =$ http://www.engineeringtoolbox.-com/dynamic-absolute-kinematic-viscosity-d_412.-html $M = v$ http://www.engineeringtoolbox.com/air-absolute-kinematic-viscosity-d_601.html
 14. Textbook Investigation of Different Airfoils on Outer Sections of Large Rotor Blades, Torstein Hiorth Soland and Sebastian Thuné 2012, Report code: MDH.IDT.FLYG.0254.2012.GN300.15HP.Ae
 15. Scott Richards, Keith Martin, and John M. Cimbala, *ANSYS Workbench Tutorial – Flow Over an Airfoil*, Penn State University Latest revision: (17 January 2011), pp1.
 16. A. Firooz and M. Gadam, Turbulence Flow for NACA 4412 in Unbounded Flow and Ground Effect with Different Turbulence Models and Two Ground Conditions: Fixed and Fixed moving ground conditions, Int. Conference on Boundary And Interior Layers BAIL 2006 (Eds), University of Gottingen, 2006.
 17. Charles D, NASA Technical Paper 2969, NASA Supercritical Airfoils: A Matrix of Family -Related Airfoils, Harris Langley Research Center, Hampton, Virginia, 1990.
 18. Richard L. Fearn, Airfoil Aerodynamics Using Panel Methods, Mathematica Journal 10:4, Wolfram Media, Inc (2008).
 19. E.M Sparrow and J. L. Gress, Technical note 4311, Prandtl number effects on unsteady forced convection heat transfer, National Advisory committee for Aeronautics, Cleveland, ohio, Washington, june 1958.
 20. IRA H. ABBOTT, ALBERT E. VON DOENHOFF and LOUIS S. STIVERS, SUMMARY OF AIRFOIL DATA NATIONAL ADVISORY COMMITTEE FOR AERONAUTICS REPORT No. 824, Langley Memorial Aeronautical, Laboratory Langley Field, Va.1945.
 21. Hamidreza Abedi, CFD with Open Source software, A course at Chalmers University of Technology Taught by H° akan Nilsson, Project work, (Nov-10-2011).
 22. *Java Foil*, Martin Hepperle, 1996-2008 Source (http://www.mh-aerotoools.de/aerfoils/jf_applet.htm)
 23. Rama Krishna N Parasaram and T N Charyulu, AIRFOIL PROFILE DESIGN BY REVERSE ENGINEERING BEZIER CURVE, ISSN 2278 – 0149. www.ijmerr.com Vol. 1, No. 3, October 2012.
 24. Helmut Sobieczky and DFVLR Gottingen, RELATED ANALYTICAL, ANALOG AND NUMERICAL METHODS IN TRANSONIC AIRFOIL DESIGN, Reprint: AIAA 79-1566 (1979).
 25. Dr. Richard Eppler, Eppler Airfoil Design and Analysis Code, Petersburg, USA.
 26. Clark y Wikipedia.
 27. J. F. Marchman and Todd D Werme , Clark y airfoil performance at low Reynolds Number, Virginia polytechnic institute and state university, Blackburg, Virginia 1-7, jan 9-12, 1984/reno, Nevada, Publisher: American institute of Aeronautics and Astronauts.
 28. Timur Dogan, Michael Conger, Maysam Mousaviraad, Tao Xing and Fred Stern, Verification and Validation of Turbulent Flow around a Clark-Y Airfoil 58:160 Intermediate Mechanics of Fluids, CFD LAB 2, Hydrosience & Engineering The University of Iowa, IA 52242-1585, p 1-54.
 29. Prof. E.G. Tulapurkara, Flight dynamics-I: Chapter-3
 30. Tanveer Chandok, Analysis of an airfoil using Computational Fluid Dynamics, Independent research thesis at the Georgia Institute of Technology, 12/17/2010, P 1- 21.
 31. Dr. Asiminia Kazakidi, Fluids dynamics software lab, second summer school on embodied intelligence," simulation and modelling within embodied intelligence. Heraklion 70013, Crete, Greece, 27 june- 1 july 2011.
 32. Robert D. Quinn and Leslie Gong, Measurement on a Hollow Cylinder at a Mach Number of 3.0 in flight boundary layer, NASA technical paper 1764, Dryden flight Research centre, Edwards, California Nov 1980, p 1-52.
 33. Christian J. Kähler, Sven Scharnowski, Christian Cierpka, High resolution velocity profile measurements in turbulent boundary layers, 16th Int

- Symp on Applications of Laser Techniques to Fluid Mechanics Lisbon, Portugal, 09-12 July, 2012, P 1-8.
34. Lelanie Smith, An interactive boundary layer modelling methodology for Aerodynamic flows, Submitted in partial fulfilment of the degree *Masters of Engineering* Department of Mechanical and Aeronautical Engineering University of Pretoria November 2011, p 1-75.
 35. D.G. Mabet and W. G. Sawyer, Experimental studies of the boundary layer on a flat Plate at mach no. 2.5 to 4.5, Procurement Executive Ministry of Defence Aeronautical Research Council, Reports and Memoranda by Aerodynamic Department, R.A.E., Bedford, London her majesty's stationary office.1976, p 1-101.
 36. Y. B. Suzen, P. G. Huang, Lennart S. Hultgren and David E. Ashpis, Predictions of Separated and Transitional Boundary Layers Under Low-Pressure Turbine Airfoil Conditions Using an Intermittency Transport Equation, Journal of Turbo machinery National Aeronautics and Space Administration, Glenn Research Centre at Lewis Field, Cleveland, OH 44135, JULY 2003, Vol. 125 / 455 (p1-10) 455-464.
 37. D. W. Holder and R. F. Cash, Experiments with a two dimensional aerofoil designed to be free from turbulent boundary layer separation at small angles of incidence for all mach numbers, reports and memoranda number 3100, Ministry of supply, N.P.L, London her majesty stationary office, august, 1957 .p.1-52.
 38. T. A. Cook, Measurement of boundary layer and wake of two aerofoil sections at high Reynolds numbers and high-subsonic mach numbers Aeronautical Research Council Reports and Memoranda, Aerodynamic Department., R.A.E., FARNBOROUGH, LONDON: Her majesty's stationary office, 1973, Reports and Memoranda number. 3722, june 1971, R.A.E. TECHNICAL REPORT 71127-A.R.C. 33 660, P 1-91.
 39. J. Hogendoorn and C Proefschrift Heat Transfer Measurements in Subsonic Transition boundary layer, (Textbook) ISBN 90-386-0550-1 NUGI831, 1997, P. 1-135.
 40. Jens M and Arne v. Johnson, MEASUREMENT IN A FLAT PLATE TURBULENT BOUNDARY LAYER, Department of Mechanics, Royal Institute of Technology. 100 44 Stockholm, Sweden. P 1-6.
 41. Dr. R. Rajappan and V. Pugazhenthii, Finite Element Analysis of Aircraft Wing Using Composite Structure, IJES, ISSN: 2319 – 1813 ISBN: 2319 – 1805, Vol2, Issue: 2, 2013, p-74-80.
 42. Tim Meyers, Ian Clark and Aurelien Borgoltz, Aerodynamic Measurement On a Wind Turbine Airfoil, *Virginia Tech, Blacksburg, VA 24061, U.S.A.*, William J. Devenport, *Virginia Tech, Blacksburg, VA 24061, U.S.A.* *Virginia Tech, Blacksburg, VA 24061, U.S.A.*, P 1-21.
 43. Galal Bahgat Salem and Mohammed Khalil Ibrahim, Measurement of Pressure Distribution over a Cambered Airfoil, Aerospace Engineering Department, Aerodynamics Laboratory – Experiment #1, Cairo University, Faculty of Engineering, April 2004, Page 1-8.
 44. Dr. Peyman Taheri NUMERICAL CALCULATION OF LIFT AND DRAG COEFFICIENTS FOR AN ELLIPSE AIRFOIL, ENSC 283 INTRODUCTION TO FLUID MECHANICS, ENSC 283 (Spring 2013), Simon fraser university.p1-5.
 45. MEHMET MERSINLIGIL, AIRFOIL BOUNDARY LAYER CALCULATIONS USING INTERACTIVE METHOD AND TRANSITION PREDICTION TECHNIQUE (Thesis), AEROSPACE ENGINEERING, SEPTEMBER 2006, p1- 113.
 46. Saso Knez, Airfoil Boundary layer, University of Ljubljana, 25 may 2005, p 1-15.
 47. NASA STI PROGRAM, NASA SP-7037 (303), April 1994.
 48. M. E. Lores, K. P. Burdges and G. D. Shrewsbury, Analysis of a Theoretically Optimized Transonic Airfoil, NASA Contractor Report 306s, Prepared for Ames Research Centre under Contract NAS2-8697, *Lockheed Georgia Company Marietta, Georgia*, NOVEMBER 1978, P 1-104.
 49. *Dan M and Somers*, EXPERIMENTAL AND THEORETICAL LOW-SPEED AERODYNAMIC CHARACTERISTICS OF A WORTMANN AIRFOIL AS MANUFACTURED ON A FIBERGLASS SAILPLANE, NASA TECHNICAL NOTE, *Langley Research Centre, Hampton, Va. 23665*, FEBRUARY 1977.
 50. P. Migliore AND S. Oerlemans, Wind Tunnel Aeroacoustic Tests of Six Airfoils for Use on Small Wind Turbines, conference paper, *AIAA Wind Energy Symposium Reno*, Contract No. DE-AC36-99-GO10337, *Nevada January 5–8, 2003-2004*, P 1-18.
 51. Philip N. Johnson-Laird, Flying bicycles: How the Wright brothers invented the Airplane, *Mind & Society* (2005) 4: 27–48 DOI 10.1007/s11299-005-0005-Received: 31 May 2004 / Accepted: 28 June 2004, Fondazione Rosselli 2005.p1-22.